Available online at www.sciencedirect.com
SCIENCE DIRECT®
Journal of Molecular Catalysis A: Chemical 228 (2005) 203–210
JOURNAL OF MOLECULAR CATALYSIS A: CHEMICAL
www.elsevier.com/locate/molcata

Density functional study of the interaction of Cu^+ ion-exchanged zeolites with H_2O and SO_2 molecules

Anibal Sierraalta[a,*], Aleida Bermudez[a], Marcos Rosa-Brussin[b]

[a] *Laboratorio de Química Computacional, Centro de Química, Instituto Venezolano de Investigaciones Científicas, Apartado 21827, Caracas 1020-A, Venezuela*
[b] *Centro de Catálisis, Petróleo y Petroquímica, Facultad de Ciencias, Universidad Central de Venezuela, Caracas, Venezuela*

Available online 5 November 2004

Abstract

In the present work, we report theoretical calculations of the interaction of H_2O, SO_2, O_2, NO_2 and NO with copper-exchanged zeolite (Cu-ZSM5). Calculations were carried out using ab initio density functional theory (DFT). The DF calculations show that the adsorption energies of NO_2 and NO are larger than the corresponding adsorption energies of water and oxygen. Therefore, neither water nor O_2 can easily displace the adsorbed NO_xs. On the contrary, water can displace adsorbed O_2 over the Cu, which indicates that the water could blocks some reaction channels of the catalytic cycle. It was also found, that the adsorption of SO_2 is not strong but can obstructs completely the active site for the reduction of the NO_x due to the formation of a $CuSO_4$ specie. The topological analysis of the molecular charge density shows that the O_2 and SO_2 molecules are activated after the adsorption over the Cu, whereas H_2O is not activated.

Keywords: Cu-ZSM5 deactivation; NO adsorption; Electronic density; Theoretical study; H_2O adsorption; SO_2 adsorption

1. Introduction

Nitrogen oxides, NO_x, are classified among the most dangerous pollutants and are responsible of the photochemical smog and acid rain. Therefore, the elimination of NO_x is one of the major challenges in environmental catalysis. The main target in these areas is the elimination of the nitrogen oxide emissions from diesel and lean-burn engines. Recently, the selective catalytic reduction (SCR) of NO_x by hydrocarbons using metal–zeolites catalysts have been considered as practical alternative for the elimination of these pollutants [1–8]. The Cu-ZSM5 catalytic system was one of the first catalysts that showed a good NO_x reduction activity. However, such system, as well as others, lacks of stability in presence of water and sulfur dioxide [1–6]. Unfortunately, engine exhausts contain large amounts of water and some amounts of sulfur dioxide, which block the reduction reaction of NO_x to N_2.

Different reasons have been given in the literature to explain such deactivation phenomenon. Cho and co-workers [7] analyzed the Cu/SUZ-4 system and proposed that the presence of H_2O and SO_2 reduces the NO_x conversion efficiency due to the blocking of the actives sites for NO_x adsorption. Fuentes and co-workers [3] studied the wet deactivation of Cu-ZSM-5 and concluded that H_2O interacts directly with Cu^{n+} sites, forming species with low or no catalytic activity. Bhatia and co-workers [6] analyzed the deactivation of Pt–Cu-ZSM5 and Cu-ZMS5 by SO_2 by means of EDAX spectrum and found evidences of sulfur adsorption on the catalyst's surface. They proposed that the SO_2 may form intermediate species such as S and H_2S which are subsequently adsorbed by the active sites of the catalyst. Additionally, it was found that, unlike the water that causes reversible deactivation, SO_2 causes irreversible damage to the catalyst. The deactivation phenomenon caused by SO_2 has also been explained through the formation of metallic sulfates on the catalytic surface [5,8]. According to Yahiro and Iwamoto [9], the reasons why the deactivation occurs in Cu-MFI are not yet very clear; for instance, CuO particles and cluster formation, or Cu^{n+} ion migration into inaccessible sites of the zeolites have all been invoked to explain the deactivation.

* Corresponding author. Tel.: +58 2 5041442; fax: +58 2 5041350.
E-mail address: asierral@ivic.ve (A. Sierraalta).

1381-1169/$ – see front matter © 2004 Published by Elsevier B.V.
doi:10.1016/j.molcata.2004.09.037

In spite of the importance of the deactivation and the experimental studies [10–15], only few theoretical calculations [16] have been performed on the Cu-ZSM5 deactivation by H_2O and SO_2. It is well-known that theoretical studies on adsorption modes, interaction energies and charge distributions are valuable tools towards the understanding of the molecular mechanisms of catalytic processes.

In the present work, the interactions of H_2O, SO_2, O_2, NO_2 and NO molecules with a Cu-ZSM5 catalyst model were studied by means of quantum chemical calculations. The paper analyzes the adsorption energies, the electronic interactions as well as the topology of the molecular charge density.

2. Models and computational details

Considering that the chemical adsorption is a highly localized phenomenon, the active site of the Cu-ZSM5 catalyst was modeled by a Cu–T3 site of a zeolite. The T3 site is a structure that has one tetragonal Al and two tetrahedral Si atom, $[H_3SiOAl(OH)_2OSiH_3]^-$. The Cu atom was set on bridge between two oxygen atoms (see Fig. 1). Similar models have been used successfully in the literature to represent one of the possible sites for the metallic ion inside the ZSM5 framework [10,12–15,17,18].

All calculations and geometry optimizations were performed at DFT level with the Gaussian 94 [19] and Spartan [20] programs. In the Gaussian 94, we employed the Becke's Three-Parameter hybrid functional [21] with Lee et al. correlation functionals [22] at unrestricted level (UB3LYP). The basis set, that explicitly includes the $(n-1)s^2$, $(n-1)p^6$, $(n-1)d^x$ and $(n)s^y$ electrons, and the relativistic effective potentials of Stevens et al. [23] were used for the Cu atom. The 6-311G(d, p) basis set was employed for the N and O atoms, while the 6-31G(d, p) basis set was used for Al, Si and H atoms. Calculations with the Spartan package were performed using the local exchange and correlation functionals

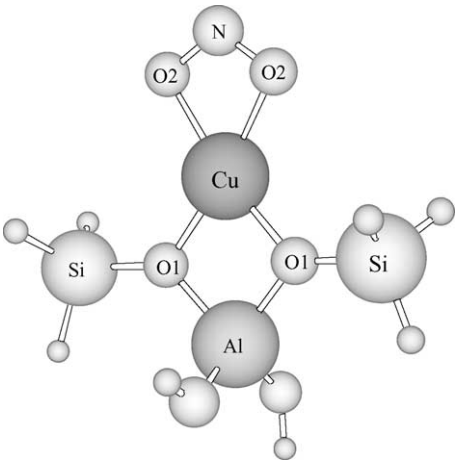

Fig. 1. Representation of the NO_2Cu–T3 molecular structures used in this work. The O1 atoms are localized along the *y*-axis. The Al and Cu atoms are in the *z*-axis.

of Slater, and Vosko et al. (SVWN) [24] with the numerical basis set DN*, which includes polarization functions on heavy atoms. We used the SVWN approach, because this methodology affords good geometries and good vibrational frequencies [18]. The SVWN approach was tested for O_2, NO, H_2O, NO_2 and SO_2 molecules. In general, the SVWN methodology reproduced quite well the experimental geometries [25]. The calculated vibrational frequencies correlate well with the experimental values. As a matter of fact, the least squares method curve-fitting reveals a nearly linear correlation with a $r^2 = 0.998$. The electronic charge distribution was analyzed using the natural bond orbital (NBO) partition scheme [26,27]. The topological properties of the electronic density of the bonds were obtained using the EXTREME program [28]. In all calculations the molecular symmetry was CS or C1, and only neutral complexes were considered.

3. Results and discussion

3.1. Model analysis

Table 1 shows the geometrical properties of the Cu–T3(S) singlet state, the Cu–T3(T) triplet state and the NO_2Cu–T3, as well as the binding energy of the NO_2 adsorption on the Cu–T3 model. Fig. 1 displays the optimal structure obtained for the NO_2Cu–T3 complex. The first step in the interaction mechanism of Cu^+ with NO_2 is the electronic rearrangement of the Cu^+ ion from a $3d^{10}$ configuration in a singlet state, Cu–T3(S), to a $3d^9 4s^1$ configuration in triplet state, Cu–T3(T) [10,15]. This electronic rearrangement is favored by the zeolite framework [10,14]. The results show that there are small geometric changes when the Cu^+ ion is promoted form a $3d^{10} \rightarrow 3d^9 4s^1$ configuration. The geometry and energy values calculated herein are in good agreement with the values reported by Sauer and co-workers [10], our previous work [14], and others [11,12,17,29]. From the data presented in Table 1 it is clear that the interaction of the NO_2 molecule with the Cu atom shortens the Cu–O1 bond distance and enlarges the N–O bond distance (N–O2) as compared to the free NO_2 molecule. The analysis of the electronic population shows that at UB3LYP level, the net charge on the Cu atom (in Cu–T3(S) model) is +0.86, which is in agreement with the expected formal charge of +1. The results show that the charge loss, results almost entirely from the 4s orbital. When the NO_2 interacts with the Cu^{1+}, a charge transfer from the metal to the NO_2 occurs. The details of the NO_2 bonding mechanism with Cu have been explained previously [14,15].

3.2. Deactivation by water

In order to study the deactivation caused by water, one H_2O molecule was allowed to interact directly with the Cu^{1+} sites, forming two conformational isomers (see Fig. 2). Both conformers exhibit similar geometric parameters (see Table 2, H_2OCu–T3(a) and H_2OCu–T3(b)), which resemble

Table 1
Bond distances and angles for Cu–T3(S), Cu–T3(T), and NO_2Cu–T3 structures (T3 = $H_3SiOAl(OH)_2OSiH_3$) at UB3LYP

Molecular system	Cu—O1 (Å)	Angle O1—Cu—O1	N—O2 (Å)	Angle O2—N—O2	O2—Cu (Å)	ΔE[a] (kcal/mol)
Cu–T3(S)	2.00	83.52				
Cu–T3(T)	1.98	78.95				
NO_2Cu–T3	1.94	80.63	1.26	110.83	2.02	42.7

Molecular system	Charge on NO_2	Charge on Cu	Cu electronic configuration
Cu–T3(S)		+0.86	$4s^{0.18}4p^{0.02}3d^{9.94}$
NO_2Cu–T3	−0.60	+1.30	$4s^{0.39}4p^{0.02}3d^{9.27}$

[a] Calculated binding energy.

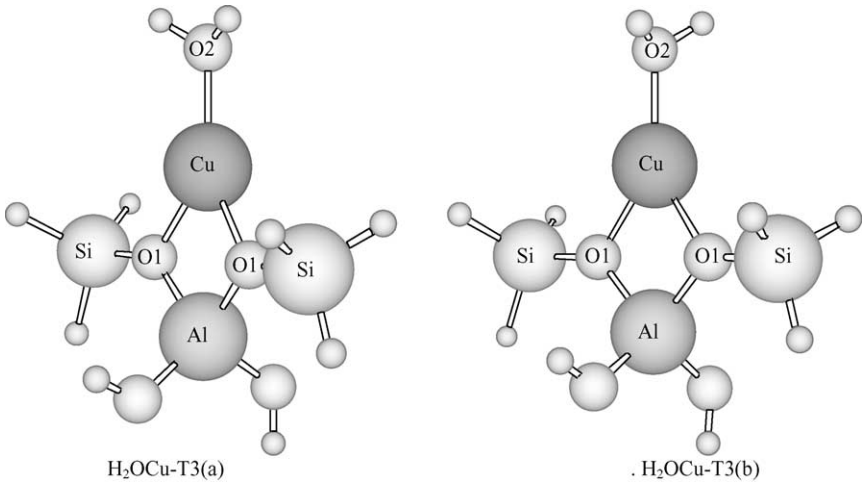

Fig. 2. Minimum energy structures of H_2OCu–T3 conformers: H_2OCu–T3(a) at the left; H_2OCu–T3(b) at the right.

Table 2
Geometries, adsorption energies (ΔE) for HO_2Cu–T3, ONCu–T3, O_2Cu–T3 systems

Molecular system	Cu—O1 (Å)	Angle O1—Cu—O1	H—O2 (Å)	Cu—O2 (Å)	Angle Cu—O2—H	Angle H—O2—H	ΔE (kcal/mol)
H_2OCu–T3(a)	2.08	78.90	0.96	1.99	119.58	107.89	26.6
H_2OCu–T3(b)	2.05	78.90	0.96	2.00	117.37	107.52	26.2
Molecular system	Cu—O1 (Å)	Angle O1—Cu—O1	N—O2 (Å)	Cu—N (Å)	Angle Cu—N—O2		ΔE (kcal/mol)
ONCu–T3(η^1-N)	1.98	80.45	1.16	1.79	148.00		31.8
Molecular system	Cu—O1 (Å)	Angle O1—Cu—O1	O3—O2 (Å)	Cu—O2 (Å)	Angle O2—Cu—O3		ΔE (kcal/mol)
O_2Cu–T3(η^2-O,O)	1.95	81.23	1.30	1.99	38.01		22.6
O_2Cu–T3(η^1-O)	1.99	80.94	1.24	1.87	131.47		16.08

the values reported by Hass and Schneider [16], who used a bigger model (Al[OSi(OH)$_3$]$_4$ = T5). In that paper, the authors reported different binding energies for two different spacial configurations, one of 21.9 kcal/mol and the other of 35.5 kcal/mol. The higher value (35.5 kcal/mol) was attributed to a contribution of a hydrogen bond between the adsorbed H_2O and a distant framework oxygen. This kind of bond is not possible in our model. Nevertheless, our calculated values of binding energy (26.6 kcal/mol) fits well with the 21.9 kcal/mol value reported by Hass and Schneider [16].

Table 3
Charges and electronic populations for HO_2Cu–T3, ONCu–T3, O_2Cu–T3 systems

Molecular system	Q_X	Q_{Cu}	dxy	dxz	dyz	dx^2-y^2	dz^2
H_2OCu–T3(a), X = H_2O	+0.07	+0.80	1.98	2.00	1.99	1.96	1.94
H_2OCu–T3(b), X = H_2O	+0.07	+0.80	1.97	2.00	2.00	1.96	1.95
ONCu–T3(η^1-N), X = NO	−0.18	+0.98	1.76	1.97	2.00	1.95	1.96
O_2Cu–T3(η^2-O,O), X = O_2	−0.44	+1.21	1.53	2.00	1.99	1.99	1.97
O_2Cu–T3(η^1-O), X = O_2	−0.21	+1.02	1.99	1.99	1.80	1.91	1.98

According to Table 3, for the NO_2 and NO cases, there is a charge transfer from the Cu to the NO_x; consequently, the Cu ion is partially oxidized. The population analysis reveals a $d^{9.9}$ configuration for Cu after interaction with water. This indicates that a $3d^{10} \rightarrow 3d^9 4s^1$ promotion is not necessary to produce a H_2O–Cu bond, as in the case of NO_x–Cu interactions [10,14,15].

According to the results presented in Table 2, the adsorption energy corresponding to H_2O molecule is lower than the one corresponding for the NO_2 or the η^1-NO bonded by the N to the Cu atom (η^1-ONCu–T3). This striking result indicates that the H_2O molecule cannot displace the NO_2 nor the NO molecule. Moreover, the results show that the following reactions:

$$H_2OCu\text{–}T3 + NO_2 \rightarrow NO_2Cu\text{–}T3 + H_2O, \quad \Delta E = -16.1\, kcal/mol \tag{1}$$

$$H_2OCu - T3 + NO \rightarrow \eta^1 - ONCu - T3 + H_2O, \quad \Delta E = -5.2 kcal/mol \tag{2}$$

are energetically favorable. It demonstrates that the NO_x species can displace the absorbed H_2O molecules. If the H_2O does not directly block the metallic site for the NO_2 or NO adsorption, it will not interfere with the reaction channels in which direct NO_x–Cu interactions exist. Therefore, the catalytic deactivation is not feasible. According to the former discussion, two chemical routes are possible to explain the deactivation by water: one, the NO_x SCR mechanism does not proceed across reaction channels only, that involve direct interactions of the NO_x with the metallic center, because reaction channels such as [29] depicted by Eqs. (3) and (4)

$$\text{zeolite–Cu} + NO_2 \rightarrow \text{zeolite–}CuO_2N \tag{3}$$

$$\text{zeolite–}CuO_2N + N_2O \rightarrow \text{zeolite–}CuO_2NO + N_2 \tag{4}$$

are not blocked by H_2O. Second, the adsorption of NO, NO_2 and H_2O proceeds by a reversible reactions and therefore, the catalytic deactivation occurs because the water is present in excess shifting, the chemical equilibrium and favoring the H_2OCu–T3 species. Table 2 shows that the H_2O as well as the NO molecules do not undergo significant geometric changes after the adsorption. The geometric parameters of the adsorbed NO specie obtained herein are in reasonable agreement with published results [16,26,30]. Nevertheless, our geometries differ from the reported by Chakraborty and co-workers [29] and Yokomichi et al. [31] (CuNO angles of 178.0° and 180.0°, respectively). Our Cu–NO binding energy (31.8 kcal/mol) is close to the values reported by other authors (41.3–51.0 kcal/mol) [16,26,31] and by Chakraborty and co-workers [29], which reported a value of 43.3 kcal/mol. The binding energy reported by Yokomichi et al. [32], 16.3 kcal/mol, is different from ours probably due to the model employed to represent the adsorption site.

3.3. Oxygen sorption

The SCR of the NO_xs occurs in presence of oxygen and the effect on the catalytic behavior appears to be complex. For example, it has been reported that the oxygen molecule inhibits the NO decomposition reaction over Cu-ZSM5 [33], nevertheless the inhibition degree decreases with temperature. The oxygen effect seems to be associated with its ability to oxidize NO to NO_2 and to prevent the reduction of Cu^{2+} [34–37]. Two types of extra-lattice oxygen atoms, α and β, have been detected by TPD chromatography [36]. The β type has been related with the generation of active sites for the NO decomposition. In the mechanism proposed in the literature, the O_2 participates in the formation of the NO_3 from NO species while the extra-lattice oxygen (ELO) aids in the formation of NO_2 from NO [27,29].

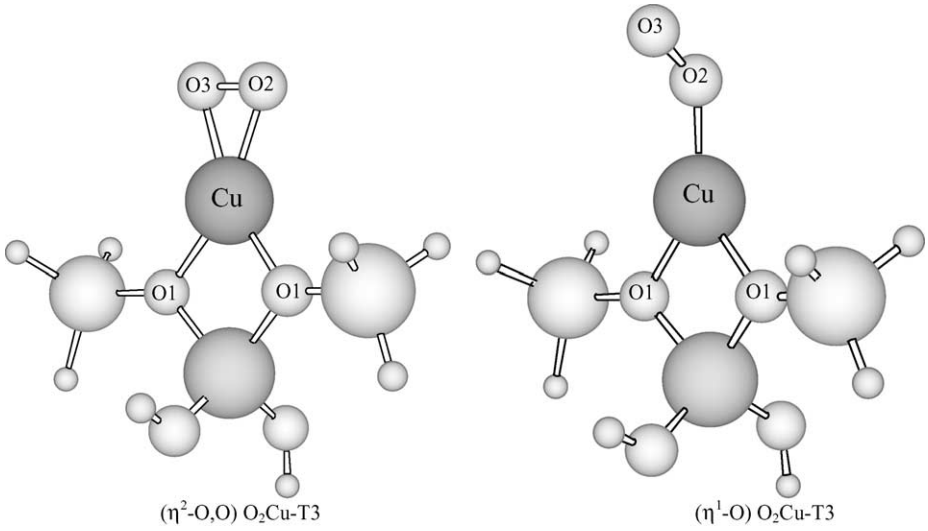

Fig. 3. Minimum energy structures for (η^2-O,O)O_2Cu–T3 and (η^1-O)O_2Cu–T3.

In order to shed some light on the effect of the oxygen, we performed quantum chemical modeling to determine how the O_2 coordinates with Cu and influences the catalytic activity. Fig. 3 shows the two minimum energy structures found in our calculations and Table 2 reports the corresponding geometries and adsorption energies. For both structures, the triplet state is the lowest energy state. The comparison of the ΔE values of the O_2Cu–T3(η^2-O,O) and O_2Cu–T3(η^1-O) structures, with the ΔE values of the H_2OCu–T3(a) and H_2OCu–T3(b) structures shows that the water competes with the O_2 for the adsorption site. The results of Table 2 seems to indicate that the following chemical equilibrium:

$$\text{zeolite–CuO}_2 + \text{H}_2\text{O} \rightleftarrows \text{zeolite–CuOH}_2 + \text{O}_2,$$

$$\Delta E = -4.0\,kcal/mol \quad (5)$$

slightly favored the formation of the H_2OCu–zeolite species. Therefore, the H_2O could block the reaction channels where the oxygen molecule participates, as for example the NO_3 formation:

$$\text{zeolite–CuO}_2 + \text{NO} \rightarrow \text{zeolite–Cu(O}_2\text{NO)} \quad (6)$$

This finding explains Chuang's experimental results [38] which show that H_2O severely inhibits the Z–Cu(NO_3) formation. Obviously, the blockage is reversible because the adsorbed water can be displaced by other molecules such as NO or NO_2. Once the water supply ceases, the NO/NO_2 molecules displace the adsorbed H_2O; thus, making the active sites available. In the catalytic cycle proposed by Bell [39], the effect of the oxygen is to diminish the NO decomposition due to the blocking of the Cu^{1+} sites and H_2O inhibition is explained by means of the formation of Cu–OH species. However, this proposed mechanism does not seem to explain the reversibility of the H_2O deactivation. The results obtained herein indicates that the reversibility can be explained in terms of the displacement of the H_2O molecule by others molecules such as the NO/NO_2. The data presented in Table 3 demonstrates that there is a charge transfer form Cu to the O_2 because the Cu is oxidized. Even though the O_2Cu–T3(η^2-O,O) and O_2Cu–T3(η^1-O) are triplet states and therefore the bonding mechanism could be similar to the NO_x–Cu bonding, there no evident electronic unpairing in the d population of the Cu atom. The spin density analysis shows that the extension of the unpaired electron localization over the O is higher than over the Cu atom (see Fig. 4). This result explains why the subsequent attack of a NO molecule to the O_2Cu–T3(η^2-O,O) or to the O_2Cu–T3(η^1-O) occurs at the O atom instead of the Cu atom. On the other hand, the molecular orbital analysis shows that the HOMO is a no-bonding orbital localized between the Cu, O2 and O3 atoms (see Fig. 3).

Table 4 shows the predicted vibrational frequencies for the adsorbed species: NO_2, H_2O, NO, and O_2. In general, the stretching frequencies of the adsorbed species are smaller than those corresponding to the free molecules, which indicates a reduction in the adsorbate's bond order. For the two H_2O adsorption modes, H_2OCu–T3(a) and H_2OCu–T3(a), the predicted stretching frequencies are similar; consequently, the experimental determination of the preferred adsorption mode should be difficult. The values calculated herein for the H–O–H bending are 1573 cm^{-1}, and 1575 cm^{-1} for H_2OCu–T3(a) and H_2OCu–T3(b). These values are close to the FTIR experimental results of 1591 and 1620 cm^{-1} reported by Konduru and Chuang [38] for the Cu-ZSM5 catalytic system treated with water steam. On the other hand, the η^1 and η^2O_2 adsorption modes present different calculated stretching frequencies (1348 and 1226 cm^{-1}) which means that it should be possible to differentiate them

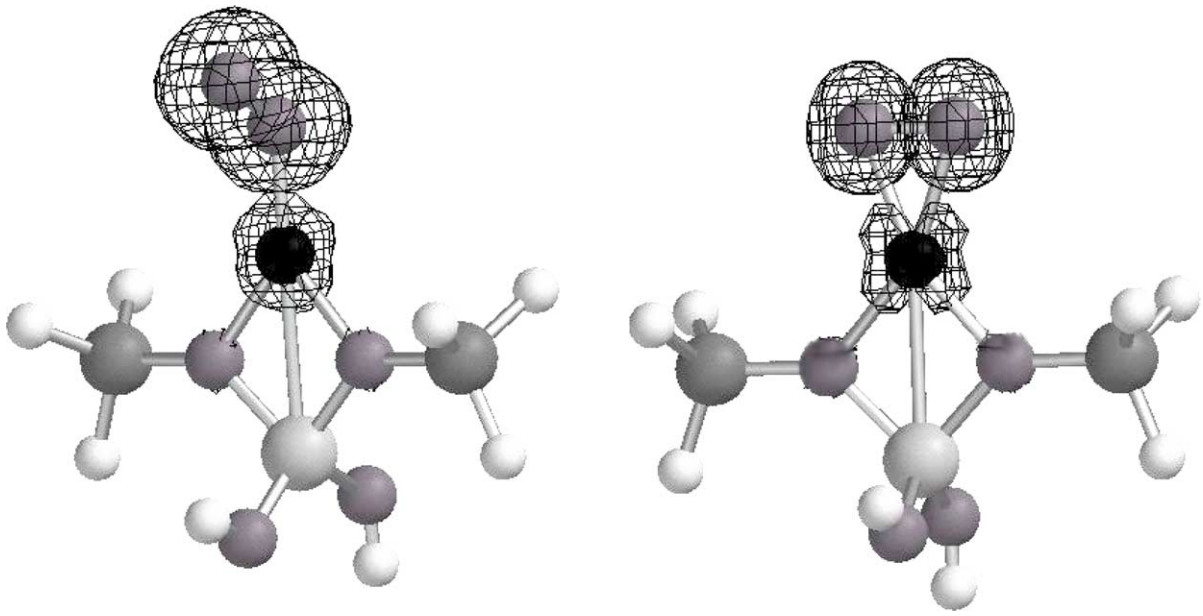

Fig. 4. (η^2-O,O)O_2Cu–T3 and (η^1-O)O_2Cu–T3 spin density surfaces.

Table 4
Predicted frequencies for NO_2, H_2O, NO and O_2 molecules adsorbed on Cu–T3[a]

Molecular system	Stretching 1 (cm^{-1})	Stretching 2 (cm^{-1})	Stretching 3 (cm^{-1})
NO_2Cu–T3	N—O = 1158 (1367)	N—O = 1282.8 (1710)	NO_2—Cu = 399
H_2OCu–T3(a)	H—O = 3577 (3610)	H—O = 3664 (3746)	H_2O—Cu = 430
H_2OCu–T3(b)	H—O = 3547	H—O = 3643	H_2O—Cu = 407
ONCu–T3(η^1-N)	N—O = 1820 (1967)		ON—Cu = 537
O_2Cu–T3(η^2-O,O)	O—O = 1226 (1577)		O2—Cu = 409
O_2Cu–T3(η^1-O)	O—O = 1348		OO—Cu = 500

[a] Computed with the linear equation of the least squares method. Values in parenthesis correspond to the free molecule.

by FTIR spectroscopy. The value for the η^2 mode is in close agreement with the theoretical value of 1150 cm^{-1} and the experimental value of 1143 cm^{-1} reported by Chakraborty and co-workers for O_2 adsorbed on transition metals [29]. Our results for the adsorbed NO stretching frequency, 1820 cm^{-1}, also agree with the experimental value of 1814–1815 cm^{-1} for the Cu^{1+}(NO)/ZSM-5 system [38,40].

Table 5 reports the topological properties (ρ_{bcp}, $\nabla^2\rho_{bcp}$, ε) of the molecular electronic density at the bond critical points (BCP) [41,14] for the LCu–T3 species (L = NO_2, H_2O, NO, O_2). From Table 5 it is clear that the topological properties of the O–Cu bond in the Cu–OH_2 complex are similar to those corresponding to the Cu–O_2N specie. The bonding with Cu affects the NO_2 more than the H_2O because there is a strong charge transfer from Cu to NO_2. The electronic density of the Cu–N bond in the η^1-ONCu–T3 system is higher than the electronic density of the Cu–OH_2 bond, which correlates with the larger binding energy found for the former system. The ellepticity of the bond ε reveals that there is a significant π participation in the bond [14,41]. The topological parameters show that the H–O bond is not activated after the adsorption. The O_2 molecule represents an interesting case. After adsorption, the bond density and the degree of local charge concentration of this molecule decrease (from 0.539 to 0.420 and −0.759 to −0.289, respectively); however, its ε value increases from 0.0 to 0.022. This means that the Cu–O_2 bond is formed at the expense of the O–O σ bond; increasing therefore the π character (increase the ε) but reducing the electronic density of the bond. This shows that the O–O bond is activated after the adsorption. For the O_2Cu–T3(η^1-O) the changes are smaller because the O_2 is bonded across one O atom.

Table 5
Topological properties of the electronic density[a] of free L and LCu–T3 specie (L = NO_2, H_2O, NO, O_2)

Molecular system	Bond	ρ_{bcp}	$\nabla^2\rho_{bcp}$	ε
Free NO_2	N—O	0.525	−1.219	0.053
NO_2 in	N—O	0.458	−1.012	0.084
NO_2Cu–T3	O—Cu	0.075	+0.326	0.102
Free H_2O	H—O	0.370	−2.003	0.031
H_2O in	H—O	0.363	−2.087	0.026
H_2OCu–T3(a)	O—Cu	0.073	+0.428	0.010
H_2O in	H—O	0.363	−2.080	0.025
H_2OCu–T3(b)	O—Cu	0.070	+0.402	0.080
Free NO	N—O	0.588	−1.965	0.090
NO in	N—O	0.571	−1.784	0.039
ONCu–T3(η^1-N)	N—Cu	0.130	+0.648	0.107
Free O_2	O—O	0.539	−0.759	0.000
O_2 in	O—O	0.420	−0.289	0.022
O_2Cu–T3(η^2-O,O)	O—Cu	0.075	+0.377	0.055
O_2 in	O—O	0.492	−0.568	0.013
O_2Cu–T3(η^1-O)	O—Cu	0.096	+0.570	0.107

[a] Values in atomic units. ρ_{bcp} is the electronic density at the bond critical point (bcp); $\nabla^2\rho_{bcp}$ the aplacian of $\rho(r)$ at the bcp; ε the bond ellipticity.

3.4. SO_x interaction

The poisoning of Cu catalysts by the SO_2 differs from the poisoning caused by water because the damage produced by the former is irreversible. In general, this phenomenon has been attributed to the $CuSO_4$ formation [5,8,42,43]. Fig. 5 displays the geometries of the three lowest energy T3CuSO_2 isomers, and Table 6 presents their net charges and adsorption energies. According to Table 6, the strongest interaction corresponds to the SO_2Cu–T3(η^1-O), followed by O_2SCu–T3(η^1-S). The SO_2Cu–T3(η^2-O,O) was obtained only at B3LYP level. The adsorption energies show that the SO_2 can displace the adsorbed O_2. Therefore, SO_2 could blocks too the same reaction channels than water. As was demonstrated above for H_2O, SO_2 can also be displaced by NO_xs (see Tables 1 and 2).

Table 6 shows that the π character of the S–O bond increases after its interaction with the metallic center; probably as a result of a reduction in the σ character of this bond. As expected, when the oxygen atoms of the SO_2 molecule interact with the Cu, the electronic density of the S–O bond decreases because now part of this electronic density participates in the Cu–O bond formation. In this sense, the S–O bond is activated by the adsorption process.

Both SO_2Cu–T3 complexes, that is, η^1-O as well as η^2-O,O, can interact with any O_2 present to produce $CuSO_4$, according to the following reactions:

$$(\eta^1 - O)SO_2Cu\text{–}T3 + O_2 \rightarrow T3\text{–}CuSO_4\,(\text{singlet}),\quad \Delta E = -172.6\,kcal/mol \tag{7}$$

$$(\eta^1 - O)SO_2Cu\text{–}T3 + O_2 \rightarrow T3\text{–}CuSO_4\,(\text{triplet}),\quad \Delta E = -169.7\,kcal/mol \tag{8}$$

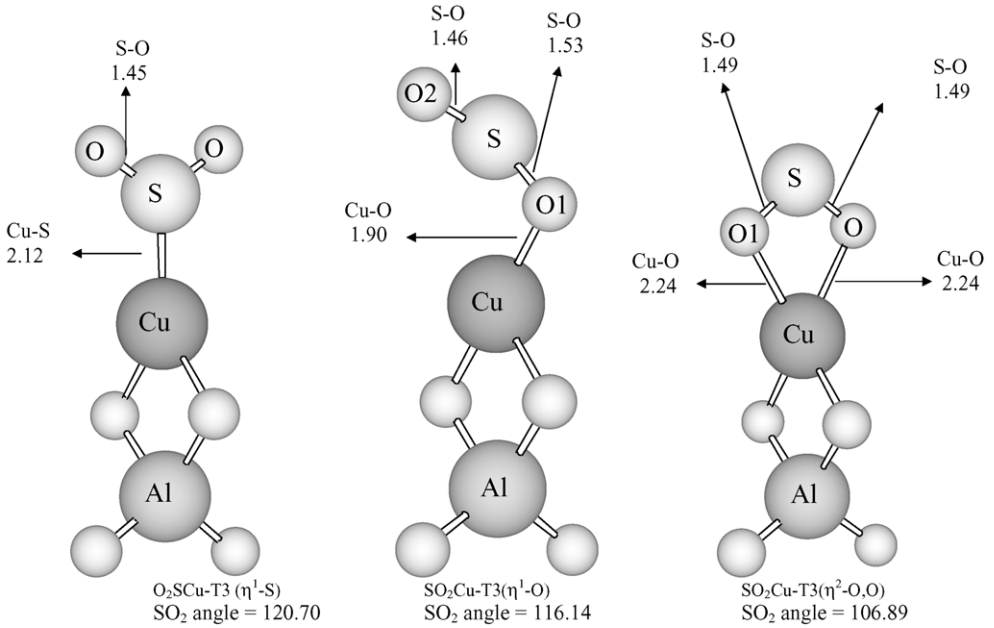

Fig. 5. O_2SCu–T3(η^1-S), SO_2Cu–T3(η^1-O) and SO_2Cu–T3(η^2-O,O) minimum energy structures. Bond lengths are given in angstroms.

Table 6
Net charges, adsorption energies (ΔE) and properties of the ρ at the bcp for SO_2Cu–T3, systems

Molecular system	Q_{SO_2}	Q_{Cu}	ΔE (kcal/mol)	ρ_{bcp}	$\nabla^2\rho_{bcp}$	ε
O_2SCu–T3(η^1-S)	−0.02	+0.81	21.9	0.097 (bond Cu—S)	0.305 (bond Cu—S)	0.257 (bond Cu—S)
				0.287 (bond S—O)	1.105 (bond S—O)	0.151 (bond S—O)
SO_2Cu–T3(η^1-O)	−0.22	+1.00	25.0	0.097 (bond Cu—O1)	0.444 (bond Cu—O1)	0.053 (bond Cu—O1)
				0.251 (bond S—O1)	0.517 (bond S—O1)	0.145 (bond S—O1)
				0.282 (bond S—O2)	1.058 (bond S—O2)	0.119 (bond S—O2)
SO_2Cu–T3(η^2-O,O)	−0.16	+0.99	17.5	0.043 (bond Cu—O1)	0.209 (bond Cu—O1)	0.128 (bond Cu—O1)
				0.269 (bond S—O1)	0.837 (bond S—O1)	0.185 (bond S—O1)
Free SO_2				0.284 (bond S—O)	1.120 (bond S—O)	0.129 (bond S—O)

$$(\eta^2-\mathrm{O,O})SO_2Cu\text{–T3} + O_2 \rightarrow \mathrm{T3\text{–}CuSO_4\,(singlet)},\quad \Delta E = -180.1\,kcal/mol \tag{9}$$

$$(\eta^2-\mathrm{O,O})SO_2Cu\text{–T3} + O_2 \rightarrow \mathrm{T3\text{–}CuSO_4\,(triplet)},\quad \Delta E = -177.21\,kcal/mol \tag{10}$$

Reactions (7) and (9) do not keep the spin because the final product as well as the reactants ((η^1-O)SO_2Cu–T3 and (η^2-O,O)SO_2Cu–T3) are singlets. Reactions (8) and (10) maintain their spin state because the final product is a triplet in both reactions. In any case, reactions (7)–(10) show that the formation of the sulfates are exothermic reactions; thus, favorable processes. Obviously, the formation of the sulfate strongly deactivates the catalyst. In general, the extend of the charge transfer from the Cu to the SO_4 moiety is higher than the one that occurs from Cu to SO_2 in the SO_2Cu–T3 complex which indicates an increase in the oxidation state of the Cu atom. The four S–O bonds in the SO_4 moiety are not equivalent. The two S–O bonds where the oxygen atoms bond to the Cu atom are longer (1.52 and 1.62 Å for the triplet and singlet states, respectively) than the remaining two free S–O bonds (1.49 and 1.44 Å for the triplet and singlet states, respectively).

4. Conclusions

The geometric parameters, electronic structures, binding energies, vibrational frequencies and topological properties of the molecular charge distribution, were determined for the Cu–T3 system and its interaction with H_2O, SO_2, O_2, NO_2 and NO molecules, using DFT. The calculated vibrational frequencies agree reasonably with the experimental values, which show, that the model mimics the catalytic site with certain degree of confidence. The theoretical results show that the interaction energy of H_2O molecule with the Cu is lower than those corresponding to the Cu–NO_2 and Cu–NO interactions, this indicates that the NO_2 and NO can displace the adsorbed H_2O molecule. Then, the chemical equilibrium

favored the formation of NO_2Cu–T3 and ONCu–T3 species and therefore, the catalytic deactivation by the water can be explained by the shifting of the chemical equilibrium, favoring the H_2OCu–T3 species. On the other hand, due to the chemical equilibrium, water can displace the adsorbed O_2; therefore it can block some reaction channels such as the NO_3 formation. These findings could account for the observed reversibility of the water deactivation. When interrupting the water supply, the NO_xs are able to displace the adsorbed H_2O and the catalytic cycle continues.

The analysis of the SO_2 interaction with the Cu–T3 complex shows that SO_2 binds stronger to Cu than O_2 but is similarly to H_2O. Therefore, SO_2 and water block the same reaction channels. Additionally, the SO_2Cu–T3 can react with oxygen to form a sulfate specie (T3–$CuSO_4$), which completely deactivates the catalyst. When the oxygen is not present, the NO_x can displace the SO_2 by a mechanism similar to the water, i.e., by a chemical equilibrium between the NO_x and SO_2 favoring the formation of the NO_2Cu–T3 and ONCu–T3 species.

The topological analysis of the molecular electron density showed that O_2 and SO_2 molecules are activated after their adsorption over Cu, undergoing a reduction of the electron density of the O–O and S–O bonds. On the contrary, the water molecule is not activated by the adsorption processes. The Cu–O bonds are similar in the O_2Cu–T3, SO_2Cu–T3 and H_2OCu–T3 complexes, with the exception that in the latter case, there is no significant π character in the bond.

Acknowledgments

The authors gratefully acknowledge CONIPET (Grant No. 97003734) and CONICIT (Grant S1-96001399) for the financial support. Dr. Ursula Ehrmann and Dr. Alejandro Arce for helpful discussions.

References

[1] J.Y. Yan, G.-D. Lei, W.M.H. Sachtler, H.H. Kung, J. Catal. 161 (1996) 43.
[2] V.I. Parvulescu, P. Grange, B. Delmon, Catal. Today 46 (1998) 233.
[3] S.A. Gómez, A. Campero, A. Martínez-Hernández, G.A. Fuentes, Appl. Catal. A: Gen. 197 (2000) 157.
[4] A. Iglesias-Juez, A.B. Hungría, A. Martínez-Arias, A. Fuerte, M. Fernandez-Garcia, J.A. Anderson, J.C. Conesa, J. Soria, J. Catal. 217 (2003) 310.
[5] G. Marban, R. Antuña, A.B. Fuertes, Appl. Catal. B: Environ. 41 (2003) 323.
[6] I.M. Saaid, A.R. Mohamed, S. Bhatia, J. Mol. Catal. A: Chem. 189 (2002) 241.
[7] A. Subbiah, B.K. Cho, J.R. Blint, A. Gujar, G. Price, J.E. Yie, Appl. Catal. B: Environ. 42 (2003) 155.
[8] W.S. Kijlstra, M. Biervliet, E. Poels, A. Bliek, Appl. Catal. B: Environ. 16 (1998) 327.
[9] H. Yahiro, M. Iwamoto, Appl. Catal. A: Gen. 222 (2001) 163.
[10] L. Rodriguez-Santiago, M. Sierka, V. Branchadell, M. Sodupe, J. Sauer, J. Am. Chem. Soc. 120 (1998) 1545.
[11] L. Rodríguez-Santiago, V. Branchadell, M. Sodupe, J. Chem. Phys. 103 (1995) 9738.
[12] X. Solans-Monfort, V. Branchadell, M. Sodupe, J. Phys. Chem. A 104 (2000) 3225.
[13] P. Nachtigall, D. Nachtigallová, J. Sauer, J. Phys. Chem. B 104 (2000) 1738.
[14] A. Sierraalta, R. Añez, M.-R. Brussin, J. Phys. Chem. A 106 (2002) 6851.
[15] A. Sierraalta, R. Añez, M.-R. Brussinc, J. Catal. 205 (2002) 107.
[16] K.C. Hass, W.F. Schneider, Phys. Chem. Chem. Phys. 1 (1999) 639.
[17] H. Soscún, O. Castellano, F. Arrieta, J. Hernandez, J. Mol. Struct. (Theochem.) 29 (2002) 592.
[18] E. Broclawok, J. Datka, B. Gil, P. Kozyra, Int. J. Mol. Sci. 3 (2002) 435.
[19] M.J. Frish, G.W. Trucks, H.B. Schlegel, P.M.W. Gill, B.G. Johnson, M.A. Robb, J.R. Cheeseman, T. Keith, G.A. Petersson, J.A. Montgomery, K. Raghavachari, M.A. Al-Laham, V.G. Zakrzewski, J.V. Ortiz, J.B. Foresman, J. Cioslowski, B.B. Stefanov, A. Nanayakkara, M. Challacombe, C.Y. Peny, P.Y. Ayala, W. Chen, M.W. Wong, J.L. Andres, E.S. Replogle, R. Gomperts, R.L. Martin, D.J. Fox, J.S. Binkey, D.J. Defrees, J. Baker, P.J. Stewart, M. Head-Gordon, C. Gonzales, J.A. Pople, Gaussian 94, Revision D.4, Gaussian, Inc., Pittsburgh, PA, 1995.
[20] Spartan 5.0, Wavefunction, Inc. http://www.wavefun.com.
[21] A.D. Becke, J. Chem. Phys. 98 (1993) 5648.
[22] C. Lee, W. Yang, R.G. Parr, Phys. Rev. B 37 (1988) 785.
[23] W. Stevens, H. Basch, M. Krauss, J. Chem. Phys. 81 (1984) 6026.
[24] S.H. Vosko, L. Wilk, Nusair, Can. J. Phys. 58 (1980) 200.
[25] National Institute of Standards and Technology of USA (NIST), Web page: http://srdata.nist.gov/cccbdb.
[26] E.D. Glendening, A.E. Reed, J.E. Carpenter, F. Weinhold, NBO Version 3.1;
A.E. Reed, L.A. Curtiss, F. Weinhold, Chem. Rev. 88 (1988) 899.
[27] W.F. Schneider, K.C. Hass, R. Ramprasad, J.B. Adams, J. Chem. Phys. B 102 (1998) 3692.
[28] F.W. Biegler-Koning, R.F.W. Bader, T.H. Tang, J. Comp. Chem. 3 (1982) 317.
[29] B.L. Trout, A.K. Chakraborty, A.T. Bell, J. Phys. Chem. 100 (1996) 17582.
[30] K.C. Hass, W.F. Schneider, J. Chem. Phys. 100 (1996) 9292.
[31] Y. Yokomichi, T. Tamabe, H. Ohtsuka, T. Kakumoto, J. Chem. Phys. 100 (1996) 14424.
[32] Y. Yokomichi, H. Ohtsuka, T. Tabata, O. Okada, Y. Yokoi, H. Ishihama, R. Yamaguchi, H. Matsui, A. Tachibana, T. Yamabe, Catal. Today 23 (1995) 431.
[33] M. Shelef, Catal. Lett. 15 (1992) 305.
[34] C. Torre-Abreu, C. Henriques, F.R. Ribeiro, G. Delahay, M.F. Ribeiro, Catal. Today 54 (1999) 407.
[35] Y. Chi, S.C. Chuang, Catal. Today 62 (2000) 303.
[36] Y. Teraoka, C. Tai, H. Ogawa, H. Furukawa, S. Kagawa, Appl. Catal. A: Gen. 200 (2000) 167.
[37] V.I. Rarvulescu, P. Grange, B. Delmon, Catal. Today 46 (1998) 233.
[38] V.M. Konduru, S.S.C. Chuang, J. Catal. 187 (1999) 436.
[39] A.T. Bell, Catal. Today 38 (1997) 151.
[40] G.T. Palomino, S. Bordiga, A. Zecchina, Phys. Chem. Chem. Phys. 1 (1999) 2033.
[41] A. Sierraalta, F. Ruette, J. Comp. Chem. 15 (1994) 313.
[42] M. Iwamoto, H. Yahiro, S. Shundo, Y. Yu-u, M. Mizuno, Appl. Catal. 69 (1991) 247.
[43] K.M. Adams, J.V. Cavataio, R.H. Hammerle, Appl. Catal. B 10 (1995) 157.